In-Stream Hydrokinetic Turbine Fault Detection and Fault Tolerant Control - A Benchmark Model

Yufei Tang¹, James VanZwieten¹, Broc Dunlap¹, David Wilson¹, Cornel Sultan², and Nikolaos Xiros³

Abstract—Increased interest in renewable energy production has created demand for novel methods of electricity production. With a high potential for low cost power generation in locations otherwise isolated from the grid, in-stream hydrokinetic turbines could serve to help meet this growing demand. Hydrokinetic turbines possess higher operations and maintenance (O&M) costs due to their isolated nature and harsh operating environment when compared with other sources of renewable energy. As such, techniques must be developed to mitigate these costs through the application of fault-tolerant control (FTC) and machine condition monitoring (MCM) for increased reliability and maintenance forecasting. Hence, the primary objective of this paper is to address a key limitation in hydrokinetic turbine research: the lack of widely available data for use in developing models by which to conduct FTC and MCM. To this end, a 20 kW research hydrokinetic turbine implemented in Fatigue Aerodynamics Structures and Turbulence (FAST) is presented and housed within the Matlab/Simulink environment. This paper details the high-fidelity simulation platform development together with the characteristics of generated data with a focus on future FTC and MCM implementation.

I. INTRODUCTION

According to the Renewable Electricity Futures Study [1], renewable electricity generation is expected to supply 80% of total U.S. electricity generation in 2050. This increasing demand for clean energy has produced a need for a wider variety of methods by which to generate electricity. As such, in-stream hydrokinetic turbine technologies have benefited from numerous innovations achieved by academia and industry over the past decade, with companies such as Verdant Power, IHI, ORPC, etc., developing hydrokinetic turbines for use in tidal, ocean-current, and river electricity production.

One of the primary barriers to the proliferation of hydrokinetic power has been reliability concerns, as the inherently harsh operating environment and isolated nature associated with these devices does not readily yield them to maintenance. The primary motivation of this research is to stimulate the development of tools and techniques by which operation and maintenance (O&M) costs can be reduced. Fault detection and isolation (FDI), fault-tolerant control (FTC), machine condition monitoring (MCM) and predictive maintenance (PdM) are all necessary means to reduce the

O&M costs of hydrokinetic turbines, and are relatively well studied and applied within the wind industry. However, as the field of hydrokinetic electricity production is relatively immature, there remains a lack of available data for use in applying these techniques in this domain. The goal of this paper is to fill this gap by developing a high-fidelity in-stream hydrokinetic turbine model for use in simulating the complex multi-physical dynamics of turbines within a stochastic hydrodynamic inflow field.

Previous marine hydrokinetic (MHK) turbine numerical simulations have been constructed to predict performance, loads, and power production, as well as for control system development and evaluation. [2] and [3] present methodologies for utilizing the Fatigue Aerodynamics Structures and Turbulence (FAST) code for accurate prediction of the hydrodynamic loads on MHK rotor blades, as well as the response of these blades to the applied loads, with a focus on predicting rotor fatigue life. However, these models do not account for controller feedback, drive-train dynamics, sensor error, or faults. Several time domain numerical simulations have been also developed by [4], [5] specifically for MHK turbine controller development. However, these numerical simulations do not include feedback from sensors or blade elasticity. Moreover, models of MHK turbine electrical power generation [6] and turbine faults [7] have been developed, but using separate numerical simulation platforms.

Over the past decade significant advancement in FTC and MCM has been made in the wind industry, while these technologies are still in infancy in the hydrokinetic domain. On the FTC side, preliminary work has been carried out in [8], [9]. Different FTC strategies have been comparatively studied in [10] for the marine current energy converter flowmeter and its generator rotor speed/position sensor failures. On the MCM side, several vibration-based approaches have been tested for the condition monitoring of MHK turbines [11], with these intrusive techniques requiring the installation of additional sensors which are also subject to failures. Recent developments for MHK turbine imbalance fault detection include data normalization and empirical mode decomposition (EMD) based methods using the generator stator current signal [12] and sparse autoencoder (SA) and softmax regression (SR) based technique using blade operating image [13]. In short, these techniques were either built using data collected from simple simulation models, dynamometer testing, or field test, which are not effective for new algorithm development, testing and validation.

Inspired from the wind turbine challenge [14], this paper employs the FAST tool [15] from the National Renewable

^{*}This work was supported by the Walter & Lalita Janke Foundation and the National Science Foundation under grant no. ECCS-1809164.

¹Y. Tang, J. VanZwieten, D. Wilson, and B. Dunlap are with Florida Atlantic University, Boca Raton, FL 33431, USA {tangy, jvanzwi, bdunlap2013, davidwilson2016}@fau.edu

²Cornel Sultan is with Virginia Tech, 460 Old Turner St., Blacksburg, VA 24061, USA csultan@vt.edu

³Nikolaos Xiros is with University of New Orleans, 2000 Lakeshore Dr., New Orleans, LA 70148, USA nxiros@uno.edu

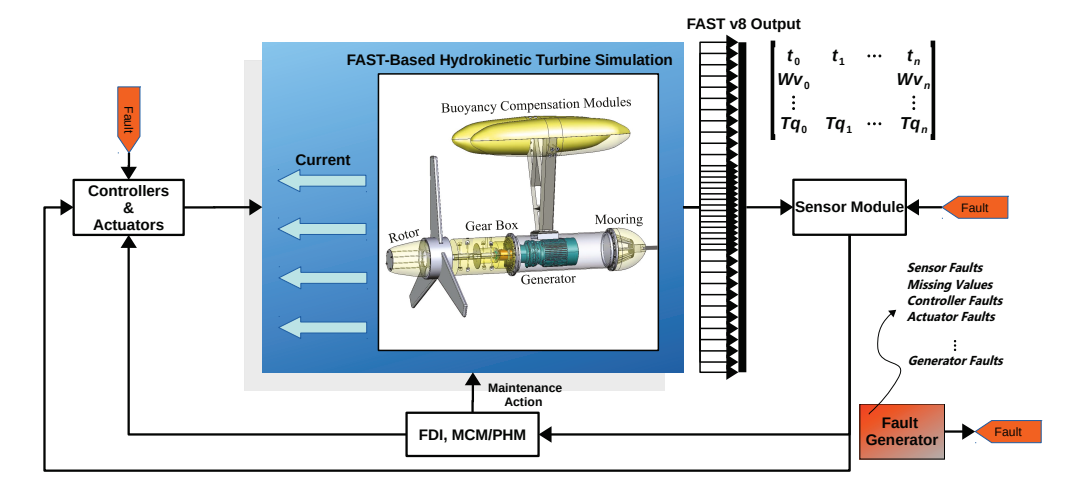


Fig. 1. FAST- and Simulink-based MCM/PHM benchmark model for in-stream hydrokinetic generation system. The 20-kW hydrokinetic turbine is simulated within the FAST-based environment, while the sensor and actuator faults are implemented within the Simulink-based environment.

Energy Laboratory (NREL) to simulate an MHK turbine. The FAST code includes a higher fidelity model of turbine structural behaviors, with up to 24 degrees of freedom. Moreover, this work differs from other models/challenges in several ways:

- A comprehensive and flexible benchmark model, comprised of a FAST-based MHK turbine, representative sensors and actuators, has been housed within a holistic Matlab/Simulink platform such that rotor blade, sensor, and actuator failures can be modeled for the assessment and validation of FTC and MCM.
- Water inflow models, generated using the TurbSim tool, have been integrated into FAST to simulate the underwater operating environments. This allows the use of more realistic "full field" water velocity inputs that vary spatially across the rotor plane and with respect to time, creating a realistic turbulent input to the turbine. Three representative conditions based on measurements made at different tidal energy sites have been modeled that have relatively mild, moderate, and high turbulent conditions.
- A recently developed turbine blade modeling approach, designed for MHK applications, has been implemented into our platform to accurately represent the interaction of MHK blades coupled with hydrodynamic and hydrostatic forcing models improving the overall validity of the simulation.

The benchmark presented in this paper is first-of-its-kind for high-fidelity MHK turbine simulation, and we predict that this work will facilitate FTC and MCM research and development in the control and MHK communities, and further help to reduce the levelized cost of energy (LCOE).

The rest of this paper is organized as follows. Section II details the benchmark model development, including a FAST preliminary, platform overview, inflow modeling, blade dynamics, sensor modeling, and actuator modeling. Section III presents faults implemented in the platform, including imbalance faults, sensor faults, and actuator faults, and Section IV concludes the paper.

II. IN-STREAM HYDROKINETIC TURBINE MODELING

The developed high-fidelity numerical simulation platform has many similarities to the 20 kW, 3-blade horizontal axis MHK turbine located at Southeast National Marine Renewable Energy Center (SNMREC) [16], [17]. In this section, we detail the overall simulation platform, TurbSim integration, underlying turbine specifications, and several other key innovations including model construction and model capabilities.

A. FAST Preliminary and Platform Overview

The latest FAST modularization framework is detailed in [18]. This framework allows for the improvement of numerical performance and flexibility, essentially creating a unified framework comprised of aerodynamic, hydrodynamic, servodynamic, and structural-dynamic modules implemented in different tool-sets which FAST "glues" together. In contrast with previous FAST versions, this new framework greatly streamlines the development and use of the toolkit, allowing for more complex systems to be modeled with reduced effort.

At its core, the simulation platform outlined in Fig. 1 relies on FAST for simulating the multibody dynamics inherent in the MHK turbine system. In this work, the AeroDyn, ElastoDyn, ServoDyn, and InflowWind modules are used with input files set using parameters from SNMREC's 20 kW MHK turbine. Stochastic turbulence models generated by NWTC's TurbSim platform, further discussed in Section II-B, provide realistic underwater operating environments. From these modules, a number of parameters can be selected as outputs to Simulink for fault-tolerant control and condition monitoring.

The FAST model is directly coupled to Simulink via the provided interface. As FAST generates output corresponding to a given time step, a sensor module, fully implemented in Simulink, feeds relevant data from the output vector into sub-blocks that emulate selected sensors. For example, a generator speed sensor is modeled by extracting the high-speed shaft rotational velocity (HSShftV) from the FAST output vector each time step which is fed into the sensor

 $\label{thm:thm:thm:equation} \mbox{TABLE I}$ Turbulence intensities and hub height current velocities at various locations.

Case	Location	TI [%]	\overline{u} [m/s]	Ref
Mild	Strangford Narrows	5	3	[19]
Moderate	Puget Sound	10	1.8	[20]
High	East River, NY	20	1.5	[21]

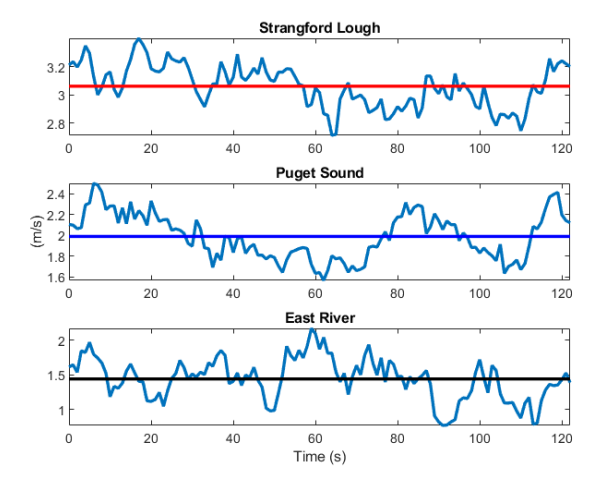


Fig. 2. Time histories of current speed and mean current velocity magnitude calculated using current inflow models for each location.

block where band-limited white noise, discrete time sampling, and discrete measurement precision are applied to form a synthesized measurement signal. The platform is highly adaptable for use in evaluating a wide variety of fault scenarios. It can be adjusted to simulate faults such as blade imbalance faults, pitch actuator faults, and a number of sensor failures limited only by the output capabilities of FAST itself.

B. Inflow Modeling

Realistic environmental characterization is important for accurately simulating MHK turbine operation. This includes accurately representing both temporal and spatial variations in the flow field. To accomplish this, a stochastic, full-field turbulence simulator called TurbSim is utilized, which calculates three-component water velocity vectors on a two-dimensional grid that is fixed in space [22]. Using Taylor's Hypothesis [23], this flow field is projected into the third spatial dimension using the mean flow speed, $V(y,z,t) \rightarrow V(x,y,z,t)$, such that correlated water velocities upstream or downstream from the rotor plane can be calculated. This is important as temporal and three dimensional spatial flow field correlation significantly impacts turbine response, and therefore signals found in generated electrical power that can mask fault signatures.

TurbSim enables the numerical simulation of water turbulence through its TIDAL-spectral model, which was developed using tidal channel data empirically derived from the Admiralty Inlet in Puget Sound, Washington [20]. As opposed to implicitly solved atmospheric boundary layer theory, this method scales its spectral amplitude and shear based on measured turbulent intensity (TI) and vertical

velocity magnitude shear $(\delta u/\delta z)$. The velocity spectra used in these models are expressed as follows:

$$S_K(f) = \sigma_K^2 s_{1,K} \left(\frac{\delta u}{\delta z}\right)^{-1} / \left(1 + s_{2,K} \left(\frac{f}{\delta u/\delta z}\right)^{\frac{5}{3}}\right)$$
(1)

where $\sigma_K^2 = U_*^2 \mu_K \exp\left(-2\pi/z_r\right)$ and z_r is the referenced hub height. The parameter $f^{-5/3}$ is a well-known fractional order representation that is used to describe the statistically invariant turbulent kinetic energy spectrum as a function of frequency [24]. Operators such as this, conveniently describe natural phenomena and are useful for converting between the frequency and time domains [25]. The parameter U_* , which represents the friction velocity, is directly proportional to TI, $U_* = TI\overline{u}$ [26]. These values are used to define the spatial coherence fraction between grid points i and j within the model as follows:

$$Coh_{i,j_k} = \exp\left(-a_k \left(\frac{r}{z_m}\right)^{C_e} \sqrt{\left(\frac{fr}{\overline{u}_m}\right)^2 + (b_k r)^2}\right)$$
 (2)

where r is the distance between i and j grid points, C_e is the coherence exponent, z_m is the mean height of these points, and \overline{u}_m is the mean current velocity at the points. Constants TI and \overline{u} are based on measurements made at each modeled tidal energy site [19]–[21], while remaining constants are left at the default TIDAL-spectral model values [27].

To represent specific tidal energy sites locations with relatively mild, moderate, and high turbulence levels, three sites targeted or utilized for hydrokinetic turbine installation and operation have been selected. A mild case with TI = 5%is located in Northern Ireland's Strangford Lough, where the 1.2 MW SeaGen project was installed [19]. These measurements were performed using an electromagnetic current meter with velocity measurements calibrated using an ADCP. To represent a moderate case of TI = 10%, ADCP and ADV data collected in the Puget Sound was referenced [20]. Finally, the study in the East River measured an average TI = 20%. The year-long study based near the Roosevelt Island Tidal Energy (RITE) project provides a high turbulence case. Table I provides model constants derived from these measurements, and Fig. 2 shows time histories of hub-height water speed, as well as hub-height mean current velocity magnitudes from each inflow model. These data provide insight by clearly showing the increasing current fluctuations as a function of TI and \overline{u} .

C. Rotor Modeling

This section focuses on the rotor modeling techniques specific to MHK turbines used in this paper. These modeling techniques are presented in detail in [28], and summarized here to help provide a complete description of the simulation platform. Both hydrodynamic and hydro-static forces are included in this model, with system response to these forces dictated by inertial, stiffness, damping and actuator characteristics, as well as controller feedback.

The simulated rotor was designed using the approach specified in [29], with the build process and hydrodynamic

characteristics summarized in [17]. Hydrodynamic forcing is calculated using lift and drag characteristics of individual hydrofoil shapes, using a Blade Element Momentum (BEM) approach that accounts for blade motion and inflow velocity field perturbations induced by the rotor [30]. Added mass forces are modeled by modifying the mass and inertia properties of the rotor blades, with hydro-static forcing introduced by modifying the gravitational constant using the relationship between net buoyant and gravitational forcing on the rotor as suggested by [2]: $g_m = gF_B/F_G$, where F_B is the total buoyant force, F_G is the total gravitational force and g is the gravitational constant.

Both flap-wise and edge-wise rotor blade bending are enabled, along with relative rotation between the rotor and generator stater accounting for the elasticity of the rotor shaft and gearbox. Rotor blade elasticity and damping values, as specified by [28], account for foam core material utilized in MHK blades but not in wind turbine blades.

D. Sensor Modeling

To ensure measurable feedback is available for FTC and MCM, turbine states output by FAST are fed through sensor models that limit sampling rates, while adding appropriate error to each data point. Values suggested for each sensor type (shown in Table II) are based on measured sensor performance, manufacturer specifications, and previous studies. Modeled sensors include IMUs (accelerometers, rate gyros and tilt/heading), water velocity sensors, torque meters, pitch angle sensors, rotor speed sensors, generator speed sensors, and electric power sensors.

The IMU model uses FAST calculated accelerations, rotation rates, tilts and heading as inputs. These variables are converted into an IMU reference frame (gravitational forcing is first included into acceleration measurements in the Inertial frame) with sensor error included. IMU update rates, as well as acceleration and rotational velocity noise levels (Table II), are set to those of an XSENSE MTi IMU [31] as suggested by [32]. This IMU's Kalman filter uses magnetic field mapping algorithms that merge 3D gyroscope, accelerometer and magnetometer data to correct for drift errors in calculated Euler outputs. Therefore, simply injecting noise into calculated attitude states is not appropriate. Instead, an approach suggested by [32] is followed where modeled rate gyro errors are converted to Euler angle rate errors, integrated, and high-pass filtered at 0.0015 Hz before being added to the calculated Euler angles.

Flow measurements are assumed to be made from a Doppler Profiler attached to the MHK turbine. Using the Doppler effect, this instrument measures water velocity upstream from the turbine. The assumed measurement location is 6 m (2 rotor diameters) upstream from the rotor at hubheight. Water velocity estimates at this location utilize Turb-Sim generated data. Assuming the velocity field is frozen allows a simple time shift, δt , to account for this separation, δx , using the mean flow velocity \overline{u} , $\delta t = \overline{u}\delta x$. Sensor error is added to these time shifted data based on the published performance of 2 MHz Aquadopp Profilers [33], assuming

TABLE II

AVAILABLE SENSORS FOR THE BENCHMARK. THESE SENSORS ARE
REPRESENTATIVE OF A KW-SCALE TESTING TURBINE.

Sensor Type	Unit	Noise Power	Rate (Hz)
Water Vel. [x/y,z]	m/s	$1.7e^{-2}/5.2e^{-2}$	1.0
Rotor Speed	rad/s	$1e^{-4}$	120
Gen. Speed	rad/s	$2e^{-4}$	120
Gen. Torque	Nm	$9e^{-1}$	120
Pitch Angle (the i-th blade)	deg/°	$1.5e^{-3}$	120
Electric Power	Watt	$1e^{+1}$	120
IMU (acc, x/y/z)	m/s^2	$[8.1/8.5/8.5]e^{-3}$	100
IMU (rot vel, x/y/z)	rad/s	$[5.5/6.0/5.1]e^{-3}$	100
IMU (Euler, $\phi/\theta/\psi$)	rad	NA	100

data is collected at 1 Hz using 1 m bins while pinging as quickly as possible for an 8 m range. Errors associated with rotor and generator rotational velocity, generator torque, and generated electrical power measurements are set to values suggested by [14].

E. Actuator Modeling

Actuator models for the generator and blade pitch are utilized in this benchmark simulation.

Generator Actuator Model: FAST can simulate generators inside the ServoDyn module. However, the electrical system and its controllers in the hydrokinetic turbine have much faster dynamics making it necessary to consider the generator control loop separately from the turbine control loop due to time constant separation [34]. Generator dynamics and generated power have been modeled in the Simulink environment using the following relationships:

$$\begin{cases}
\tau_g(s)/\tau_{g,r}(s) = \alpha_{gc}/(s + \alpha_{gc}) \\
P_g(t) = \eta_g \omega_g(t)\tau_g(t)
\end{cases}$$
(3)

where α_{gc} depends on the capacity of the generator, which has been set as $\alpha_{gc}=20$ corresponding to the 20 kW research MHK turbine; and η_g is the efficiency of the generator, which has been set as $\eta_g=0.98$.

While this generator model is quite simplistic, it adequately represents most generator topologies for the model resolution and selected faults in this paper [14]. Moreover, since this has been modeled in the Simulink environment, it can be easily extended to model more complex generators, such as the permanent magnet synchronous generator (PMSG) shown in [35].

Pitch Actuator Model: The hydraulic pitch system is modeled as a closed loop, second order transfer function from the pitch angle reference β_r to the actual pitch angle β as:

$$\frac{\beta(s)}{\beta_r(s)} = \frac{\omega_n^2}{s^2 + 2\zeta\omega_n s + \omega_n^2} \tag{4}$$

where ζ is the damping factor and ω_n is the natural frequency. A transfer function is associated with each of the three pitch systems, which are identical when no fault exists. Similarly to [14], for the no fault case, we use the parameters $\zeta=0.6$ and $\omega_n=11.11$. In addition, constraints on the pitch actuator include the pitch angle being restricted to the interval -2° to 90° deg and the pitch rate being restricted to the interval -8° /s to 8° /s.

 $\label{thm:limbalance} \textbf{TABLE III}$ Imbalance, sensor and actuator fault scenarios.

Fault No.	Fault Description	Fault Type	
Blade Fault 1	Pitch Imbalance	Offset	
Blade Fault 2	Mass Imbalance	Offset	
Sensor Fault 1	Water Vel. Sensor	Missing/Error Scaling	
Sensor Fault 2	Generator Speed Sensor	Scaling	
Sensor Fault 3	Generator Power Sensor	Scaling	
Sensor Fault 4	Pitch Angle Sensor	Stuck	
Sensor Fault 5	IMU	Offset	
Actuator Fault 1	Pitch Actuator	Change in Dynamics	
Actuator Fault 2	Generator Torque	Offset	

III. FAULT DESCRIPTION

Blade faults account for approximately 13% of failures and 9% of total downtime experienced for maintenance and repairs, while sensor and control system faults combined account for 27% of failures and 24% of downtime experienced in wind turbines [36]. These metrics will likely increase for MHK turbines due to their harsh underwater operating environments. Therefore, the platform has simulated scenarios corresponding to blade imbalance, sensor and actuator faults.

A. Blade Faults

Blade imbalances usually arise either as a result of defects that occur during the manufacturing and construction phases of the turbine and its parts, manifest themselves slowly over time due to simple wear and tear, or are the result of a traumatic event. Imbalance faults typically fall into two categories, pitch (hydrodynamic) imbalance faults, where hydrodynamic loading is blade dependent, and mass imbalance faults, where the mass properties of the blades are not consistent (Blade Faults 1 and 2 in Table III). Blade imbalances have the ability to induce large dynamic loads and vibrations on the rotor shaft that interfere with the shaft's natural operating frequency.

- Pitch imbalance fault: This fault occurs when the pitch angle of a single rotor blade is offset from the others, which is modeled by including an offset into the pitch of one rotor blade within FAST. This results in unbalanced hydrodynamic loading, with a forcing frequency equal to the blade rotation rate. These fluctuations primarily occur in the downstream and torsional direction, directly affecting the dynamics of the system. As an example, both power production and bearing loads are directly impacted by this fault, as shown in Fig. 3. Four cases have been considered with values of 5, 10, 15 and 20°.
- Mass imbalance fault: This fault occurs when the mass of one rotor blade differs from the others, which will most likely occur due to bio-fouling or water intrusion. This fault can be modeled by increasing the mass properties of a single blade. This will induce an unbalanced torque on the rotor hub caused by gravitational forcing, as well as an unbalanced radial force due to centripetal acceleration. Both of those forcing functions will cyclically occur at the rotor rotation rate. Four cases have been considered with the mass of one blade increased by 5, 10, 15 and 20% of its original mass.

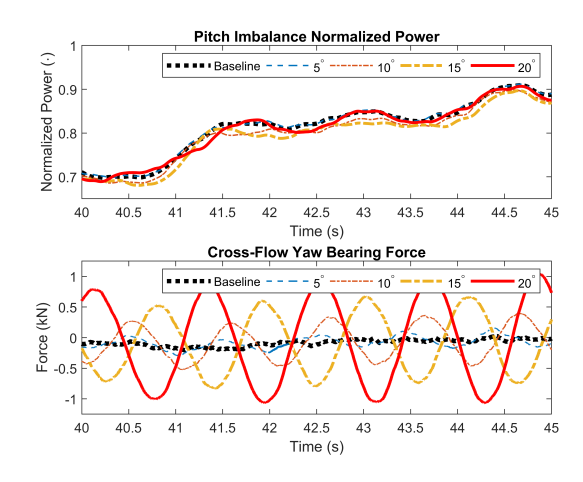


Fig. 3. Generated power and cross-flow bearing force resulting from a single blade pitch offset of 5, 10, 15, and 20° .

B. Sensor and Actuator Faults

Sensors faults include measurements that are "stuck," "scaled" from the true values, "offset" from the true values, "missing" measured feedback and "error scaling", as indicated for Sensor Faults 1-5 in Table III, and with an example shown in Fig. 4. Actuator faults are associated with actuators used by the turbine blade pitch drives and generator torque, which are indicated by Actuator Faults 1 and 2 in Table III.

- Water velocity sensor fault: Two cases have been considered in the velocity sensor fault. Measurement noise levels doubled (error scaling) due to low levels of particulate in the water (or sensor bio-fouling), and a more severe case where water velocity measurements are missing.
- Generator speed sensor fault: The speed sensor fault causes the generator speed measurement to be scaled by a factor of 0.95.
- Generator power sensor fault: While power sensor fault is occurring, the measured generator power is scaled with a factor of 1.1.
- Pitch angle sensor fault: This fault results in one blade having a stuck pitch angle sensor, which holds a constant value of 5°.
- IMU sensor fault: This fault results in an offset of -0.5 m/s² on the tower top accelerometer in both the fore-aft and side-to-side directions.
- Pitch actuator fault: There are two types of pitch actuator faults, abrupt and slow change in dynamics caused by hydraulic power drop and increased air content, respectively. These two types of fault are modeled by changing the parameters ζ and ω_n in the relevant pitch actuator model in Equ. (4). The two parameters for the pressure drop case are denoted as $\zeta=0.45$ and $\omega_n=5.73$ and the two parameters for the increased air content model are denoted as $\zeta=0.09$ and $\omega_n=3.42$.
- Generator torque fault: This fault indicates an offset on the generator torque, which can be caused by an error in the initialization of the converter controller. In this benchmark, the offset has been set to 100 Nm.

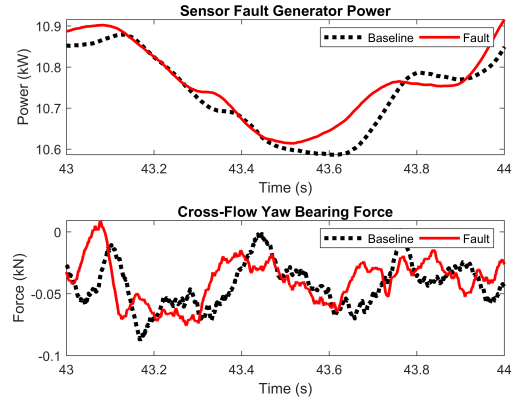


Fig. 4. Effects of a faulty generator speed sensor on turbine dynamics.

IV. CONCLUSIONS

In this paper, we have presented a benchmark model for use in designing and testing FTC and MCM algorithms for in-stream hydrokinetic turbines *. This model is high-fidelity, using well-recognized FAST code with redeveloped modules to better represent the underwater environments. Blade, sensor and actuator faults have been provided and discussed to better reflect the state-of-the-art of the hydrokinetic industry.

REFERENCES

- [1] "Renewable Electricity Futures Study, Department of Energy," https://www.nrel.gov/analysis/re-futures.html, accessed: 2018-09-10.
- [2] F. Zhou, H. Mahfuz, G. M. Alsenas, and H. P. Hanson, "Static and fatigue analysis of composite turbine blades under random ocean current loading," *Marine Technology Society Journal*, vol. 47, no. 2, pp. 59–69, 2013.
- [3] T. Suzuki and H. Mahfuz, "Analysis of large-scale ocean current turbine blades using FluidStructure Interaction and blade element momentum theory," Ships and Offshore Structures, Jan. 2018.
- [4] J. H. VanZwieten, N. Vanrietvelde, and B. L. Hacker, "Numerical Simulation of an Experimental Ocean Current Turbine," *IEEE Journal* of Oceanic Engineering, vol. 38, no. 1, pp. 131–143, Jan. 2013.
- [5] P. Pyakurel, J. H. VanZwieten, C. Sultan, M. Dhanak, and N. I. Xiros, "Numerical simulation and dynamical response of a moored hydrokinetic turbine operating in the wake of an upstream turbine for control design," *Renewable Energy*, vol. 114, pp. 1134–1145, 2017.
- [6] V. Tzelepis, J. H. VanZwieten, N. I. Xiros, and C. Sultan, "System modeling and simulation of in-stream hydrokinetic turbines for power management and control," *Journal of Dynamic Systems, Measurement, and Control*, vol. 139, no. 5, p. 051005, 2017.
- [7] N. Vanrietvelde, "Numerical performance prediction for FAUs first generation ocean," Master's thesis, Florida Atlantic University, 2009.
- [8] T. D. Ngo, C. Sultan, J. H. VanZwieten, and N. I. Xiros, "Variance constrained cyclic blade control of moored ocean current turbines," in *American Control Conference (ACC)*, 2016. IEEE, 2016, pp. 6622– 6627.
- [9] —, "Model predictive control for moored ocean current turbines," in *American Control Conference (ACC)*, 2017. IEEE, 2017, pp. 875–880.
- [10] H.-T. Pham, J.-M. Bourgeot, and M. E. H. Benbouzid, "Comparative investigations of sensor fault-tolerant control strategies performance for marine current turbine applications," *IEEE Journal of Oceanic Engineering*, 2017.
- [11] R. D. Wald, Vibration analysis for ocean turbine reliability models. Florida Atlantic University, 2012.
- [12] M. Zhang, T. Wang, T. Tang, M. Benbouzid, and D. Diallo, "An imbalance fault detection method based on data normalization and emd for marine current turbines," *ISA transactions*, vol. 68, pp. 302– 312, 2017.
- *Available at https://github.com/YufeiTang/MHK. A special session is planned to accommodate papers from this benchmark challenge.

- [13] P. Wen, T. Wang, B. Xin, T. Tang, and Y. Wang, "Blade imbalanced fault diagnosis for marine current turbine based on sparse autoencoder and softmax regression," in *The 33rd Youth Academic Annual Confer*ence (YAC). IEEE, 2018, pp. 246–251.
- [14] P. F. Odgaard and K. E. Johnson, "Wind turbine fault detection and fault tolerant control - an enhanced benchmark challenge," in *American Control Conference (ACC)*, 2013. IEEE, 2013, pp. 4447–4452.
- [15] "FAST," https://nwtc.nrel.gov/FAST, accessed: 2018-06-05.
- [16] F. R. Driscoll, G. M. Alsenas, P. P. Beaujean, S. Ravenna, J. Raveling, E. Busold, and C. Slezycki, "A 20 KW open ocean current test turbine," in OCEANS 2008, Sep. 2008.
- [17] M. Borghi, F. Kolawole, S. Gangadharan, W. Engblom, J. VanZwieten, G. Alsenas, W. Baxley, and S. Ravenna, "Design, fabrication and installation of a hydrodynamic rotor for a small-scale experimental ocean current turbine," in 2012 Proceedings of IEEE Southeastcon. IEEE, 2012.
- [18] J. Jonkman, "The new modularization framework for the FAST wind turbine CAE tool," in 51st AIAA Aerospace Sciences Meeting including the New Horizons Forum and Aerospace Exposition, 2013, p. 202.
- [19] J. MacEnri, M. Reed, and T. Thiringer, "Influence of tidal parameters on seagen flicker performance," *Phil. Trans. R. Soc. A*, vol. 371, no. 1985, p. 20120247, 2013.
- [20] J. Thomson, B. Polagye, V. Durgesh, and M. C. Richmond, "Measure-ments of turbulence at two tidal energy sites in Puget Sound, WA," *IEEE Journal of Oceanic Engineering*, vol. 37, no. 3, pp. 363–374, 2012.
- [21] Y. Li, J. A. Colby, N. Kelley, R. Thresher, B. Jonkman, and S. Hughes, "Inflow measurement in a tidal strait for deploying tidal current turbines: lessons, opportunities and challenges," in ASME 2010 29th international conference on ocean, offshore and arctic engineering. American Society of Mechanical Engineers, 2010, pp. 569–576.
- [22] B. Jonkman and L. Kilcher, "TurbSim Users Guide: Version 1.06.00," National Renewable Energy Laboratory, Technical Report NREL/TP-xxx-xxxx, 2012. [Online]. Available: https://nwtc.nrel.gov/ system/files/TurbSim.pdf
- [23] A. Platt, B. Jonkman, and J. Jonkman, "Inflowwind users guide," Technical Report, CO, USA, National Wind Technology Center, Tech. Rep., 2016.
- [24] U. Frisch and A. Kolmogorov, Turbulence: the legacy of AN Kolmogorov.
- [25] C. A. Monje, Y. Chen, B. M. Vinagre, D. Xue, and V. Feliu-Batlle, Fractional-order systems and controls: fundamentals and applications. Springer Science & Business Media, 2010.
- [26] MIT Course, "Basics of turbulent flow, Fact Sheet N°282," 2017, http://www.mit.edu/course/1/1.061/www/dream/SEVEN/ SEVENTHEORY.PDF.
- [27] "Marine hydrokinetics nwtc information portal," https://nwtc.nrel.gov/technology-type/marine-hydrokinetics.
- [28] T. Suzuki and H. Mahfuz, "Analysis of large-scale ocean current turbine blades using fluid–structure interaction and blade element momentum theory," *Ships and Offshore Structures*, vol. 13, no. 5, pp. 451–458, 2018.
- [29] J. H. VanZwieten, C. M. Oster, and A. E. Duerr, "Design and analysis of a rotor blade optimized for extracting energy from the florida current," in ASME 2011 30th International Conference on Ocean, Offshore and Arctic Engineering. American Society of Mechanical Engineers, 2011, pp. 335–341.
- [30] J. Jonkman, G. Hayman, B. Jonkman, and R. Damiani, "Aerodyn v15 users guide and theory manual," NREL Draft Report, 2015.
- [31] MTi and MTx User Manual and Technical Documentation.
- [32] M. T. Young, Design and analysis of an ocean current turbine performance assessment system. Florida Atlantic University, 2012.
- [33] E. A. Nystrom, K. A. Oberg, and C. R. Rehmann, "Measurement of turbulence with acoustic doppler current profilers-sources of error and laboratory results," in *Hydraulic Measurements and Experimental Methods* 2002, 2002, pp. 1–10.
- [34] F. A. M. Vásquez, T. F. de Oliveira, and A. C. P. B. Junior, "On the electromechanical behavior of hydrokinetic turbines," *Energy Conversion and Management*, vol. 115, pp. 60–70, 2016.
- [35] X. Gong and W. Qiao, "Simulation investigation of wind turbine imbalance faults," in *Power System Technology (POWERCON)*, 2010 International Conference on. IEEE, 2010, pp. 1–7.
- [36] J. Ribrant and L. Bertling, "Survey of failures in wind power systems with focus on Swedish wind power plants during 1997-2005," in *Power Engineering Society General Meeting*, 2007. IEEE. IEEE, 2007.